# Direct Imaging of Cu Dimer Formation, Motion, and Interaction with Cu Atoms on Ag(111)

Karina Morgenstern, Kai-Felix Braun, and Karl-Heinz Rieder
*Institut für Experimentalphysik, FB Physik, Freie Universität Berlin, Arnimallee 14, D-14195 Berlin, Germany*
(Received 25 February 2003; published 28 July 2004)

We have investigated the formation and motion of copper adatoms and addimers on Ag(111) between 6 and 25 K with low-temperature scanning tunneling microscopy. The presence of atoms and dimers alters the motion of atoms and dimers via the long-range interaction mediated by the electrons in the two-dimensional surface state band. Above 16 K, dimers show quantum rotor behavior with altered rotational behavior in the presence of an additional adatom. The most favorable diffusional motion of the dimer is identified in combination with molecular dynamics calculations to be a zigzag out-of-cell motion starting above 24 K.

DOI: 10.1103/PhysRevLett.93.056102 PACS numbers: 68.35.Fx, 68.37.Ef, 68.55.Jk, 73.20.–r

Our present understanding of the surface diffusion of adparticles on metal surfaces and their mutual interaction is far from being complete, though this knowledge is essential for a detailed understanding of numerous surface phenomena such as melting, roughening, crystal and film growth, catalysis, and corrosion. A comprehensive picture that connects diffusional properties on the atomic level with macroscopic patterns such as growth modes requires deep insight into motion and aggregation of adparticles starting from monomers. Thus, numerous experiments and accurate theoretical calculations have addressed the diffusion of single adatoms [1,2], which then served as sole input to describe surface diffusion [3,4]. Only a few studies have dealt with the properties of dimers [5–8] or even larger adparticles [9]. However, theory suggests dimer diffusion to be of utmost importance, e.g., for mass transport [10] and for step bunching instabilities during growth [11]. State-of-the-art theory has shown that a complete characterization of adparticle diffusion is more complicated than that of adatoms already for the case of dimers [12]. This study has suggested intracell and intercell motion. For intracell motion, the dimer is confined to the small hexagonal cell of six sites around a given surface atom (called quantum rotor).

Interactions of different character depend on the adparticle distance [13]. At small separation, direct electronic interactions prevail leading to localized chemical bonds [14], i.e., to dimers or larger adparticles. For surfaces with occupied surface states adsorbate interactions can be mediated indirectly via Friedel-type interactions [15]. The surface state electrons influence adatom motion at low temperature by modifying the diffusion potential in an oscillatory form [16]. Scanning tunneling microscopy (STM) measurements revealed strong effects on surface morphology due to these indirect oscillatory interactions for copper adatoms on Cu(111) [16]. The number of STM studies on metals that determine reliable activation energies by directly observing adatom diffusion is very small [16–18].

In this Letter, we give a complete account of dimer formation and motion for the heteroepitaxial case of copper on Ag(111). We have directly observed atom motion, dimer formation, intercell and intracell motion of dimers, and interaction between atoms and dimers between 6 and 25 K with a low-temperature STM. The activation energy of adatom and dimer intercell motion is $(65 \pm 9)$ meV and $\sim$73 meV, respectively. The most favorable diffusional motion of the dimer is identified as a zigzag out-of-cell motion. Adatom and dimer motion change in the presence of other atoms and dimers. For dimers, the quantum rotor behavior above $T \approx 16$ K is altered in the presence of an additional adatom. In the case of dimer-to-adatom interaction a long-range oscillatory distance distribution is found over several tens of nanometers. The observed behavior impedes the formation of trimers and thus has important consequences for growth. Our study constitutes a model system for dimers on metal surfaces. For generalization we compare the results with molecular dynamics simulations for both the heteroepitaxial and the homoepitaxial case and point out quantitative differences.

The experiments are performed in ultrahigh vacuum with a low temperature STM [19]. The single crystalline Ag(111) surface is cleaned by sputtering and annealing cycles. Copper is deposited onto the surface within the STM at 7 K. Measurements are performed between 6 and 25 K. Special care has been taken that imaging does not influence the data [20]. Images are recorded at regular time intervals between 45 and 200 s at temperatures between 6 and 25 K in order to follow the diffusion of atoms and dimers. Above this temperature single atoms attach to steps or form larger adparticles.

To understand the atomistic processes underlying the motion, we have performed molecular dynamics calculations of activation energies using the semiempirical effective medium theory (EMT) potentials. EMT is well suited when fast and simple calculations are needed to elucidate overall trends behind observed effects and give insight into the dominating mechanism for a variety of elementary processes [21].

Figure 1(a) shows the surface directly after deposition. Two types of protrusions are discernible. The circular

  

protrusions with an apparent height of 40 pm at 100 mV and a FWHM of 0.42 nm (with the sharpest tips) are atoms. The ellipsoidal protrusions with an apparent height of 65 pm at 100 mV and a FWHM of 0.62 and 0.48 nm along their long and short axes, respectively, are dimers as verified by direct observation of dimer formation [Fig. 1(b)]. Dimer formation is observed above 19 K on the experimental time scale.

Around adsorbates, the standing wave patterns of the electrons in the surface state band can be directly imaged at low biases. The standing wave pattern around the ellipsoidal dimer is only slightly ellipsoidal [Fig. 1(c)] with an aspect ratio of 1.06. The smaller diameter is close to the one around an isolated atom.

Adatom motion is first observed at 19 K on the experimental time scale. Figure 2(a) shows snapshots of a 8 h STM movie recorded at 21.5 K [22]. The atoms move predominantly by lattice constant distances [Fig. 2(b)] indicating hops between equivalent (fcc or hcp) sites. From the occupation probability of the two inequivalent sites we deduce an energy difference of $(5.5 \pm 1.0)$ meV [23]. From the adatom diffusivity, we determine the activation energy of diffusion to $(65 \pm 9)$ meV [Fig. 2(c)]. The molecular dynamics (MD) simulations give an adatom diffusion barrier of 80 meV (disregarding the indirect interactions via surface states).

Dimers perform intracell motion by changing between three equivalent sites [marked with R, L, and H in Fig. 2(a)], thus rotating around their central surface atom. Therefore, the center of mass jump distance of the dimer is only a fraction of the lattice spacing [Fig. 2(b)]. On the experimental time scale, dimer rotation is observed above 16 K and dimer intercell (i.e., out-of-cell) motion above 24 K [Fig. 2(d)]. The latter motion has a probability of $\approx 5.5 \times 10^{-4}$/s at 24 K, which corresponds to an activation energy of $\approx 73$ meV assuming a prefactor of $10^{12}$/s.

The adatom motion at elevated temperatures leads to a redistribution of the initially random distance distribution showing now oscillations as expected for an oscillatory potential [Figs. 3(a)–3(c)]. An increased denuded zone around the atom comprises around six atomic distances. The oscillation is far more obvious in the distance distribution of adatoms to dimers [Fig. 3(b)] where seven minima are observed, the last one at a distance of 23.1 nm. The minima wash out with increasing temperature, but the first minimum is still visible in the dimer-to-adatom distribution at 24 K [Fig. 3(c)]. The denuded zone implies that at least up to this temperature trimer formation is obstructed and the growth mode is influenced.

To identify the underlying process of the dimer motion, we calculated the energy barriers for both the heteroepitaxial [i.e., Cu/Ag(111)] and the homoepitaxial [i.e., Cu/Cu(111)] case for several intracell and intercell motion types. The most relevant ones are shown in Figures 4(a)–4(f) in comparison to previous calculations

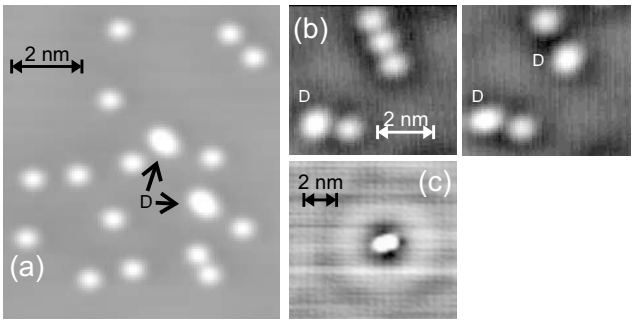


FIG. 1. (a) STM image of Cu on Ag(111) (7.5 K, 210 mV, 0.82 nA), (b) dimer formation, $\Delta t = 100$ s (19 K, 203 mV, 0.43 nA), and (c) standing wave pattern around dimer (0.095 mV, 2.3 nA).

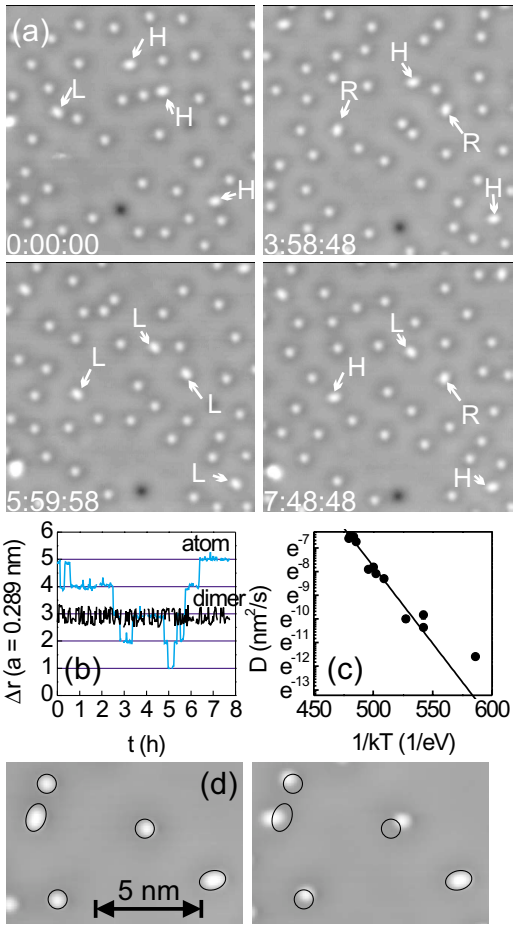


FIG. 2 (color online). (a) Time lapse sequence of adatom and dimer motion, letters R (right inclined), L (left inclined), and H (horizontal) mark dimer positions (21 K, 203 mV, and 0.43 nA); the total film consists of $N = 262$ images; $\Delta t = 100$ s. (b) Position change of adatom and dimer in time; the horizontal lines denote atomic surface distance. (c) Arrhenius plot of adatom diffusivity D; the linear fit has a prefactor of $6 \times 10^{-10}$ nm$^2$/s. (d) Dimer intercell motion (24 K; 200 mV, and 0.4 nA) $\Delta t = 80$ s; the positions of the circles and of the ellipse are identical in the two images and serve to guide the eye.

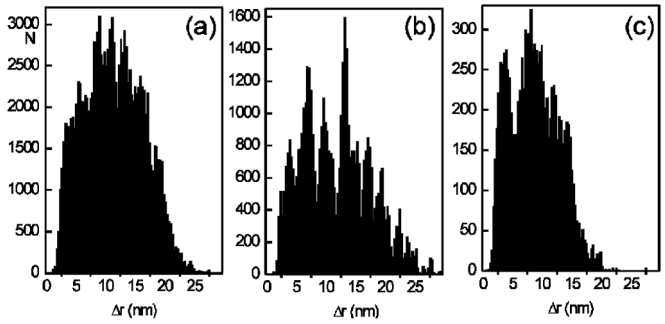


FIG. 3. Distance distribution upon adatom motion (a),(b) at 21.5 K and (c) at 24 K (a) between atoms and (b),(c) between atoms and dimers.

for Ir/Ir(111) based on embedded atom calculation [24] and Al/Al(111) based on first-principles calculation [12]. For the heteroepitaxial intracell motion, we find only insignificant differences for sequential (a,b) and collective (c) rotational motion and collective hopping (d). Thus, we cannot identify the underlying process. In contrast, collective rotational motion for the two homoepitaxial cases, Al/Al(111) [12] and Cu/Cu(111), require more than twice the activation energy. A possible explanation is the large lattice mismatch between silver and copper leading to a copper bulk distance for the copper dimer in the heteroepitaxial case.

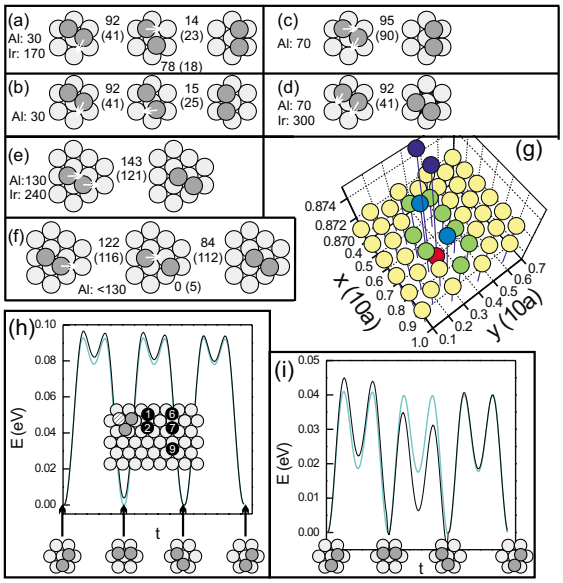


FIG. 4 (color online). MD results for dimer motion: (a)–(f) values in meV for the Cu dimer on Ag(111) [Cu(111)]. (a),(b) Sequential rotation, (c) collective rotation, (d) collective intracell hopping over the bridge site, (e) collective intercell hopping over the bridge site, (f) sequential intercell motion, (g) out-of-place displacement of an atom around a dimer (black); surface plane at $z = 0.872$; unit: atomic surface distance $a = 0.289$ nm, and (h),(i) the dimer (gray) rotates with a third atom (black) close by (black line for position 2) as compared to normal rotation (gray line). Different positions of an additional atom are marked: the horizontal axis is the simulation time axis; the ball model indicates the corresponding dimer configurations; (h) Cu/Ag(111) and (i) Cu/Cu(111).

With 122 meV the dimer zigzag motion is lowest in energy for intercell motion [Fig. 4(f)]. Intercell motion is considerably higher in energy than intracell motion due to an out-of plane displacement of surface atoms around the dimer [Fig. 4(g)] which has to be transferred to neighboring surface atoms upon dimer intercell motion: For a copper dimer on Ag(111) [Cu(111)], we find that the topmost layer is contracted inwards by 1.6 % (1.6%) of an interlayer spacing. However, the atom (dark) located below and between the dimer atoms is pushed inwards by 4.0% (3.4%). Ten other surface atoms (gray) surrounding the dimer are displaced *outwards* by up to 1.5% (0.8%).

As shown above dimers influence the adatom motion. We now tackle the following question: How do adatoms influence the dimer rotation? There are two effects, a long-range effect found in the experiment and a short-range effect found in the MD simulation. The calculation shows that the dimer rotation potential becomes asymmetric, if a monomer is positioned close by [Fig. 4(h)] due to elastic lattice deformation. This asymmetry is far more pronounced in the homoepitaxial case [Fig. 4(i)]. While a measurable asymmetry is observed only for atom positions one and two in the heteroexpitaxial case, it is still asymmetric for a distance of three lattice constants (position 7) in the homoepitaxial case. We expect a considerable increase of this asymmetry distance due to the indirect interactions via surface states in analogy to the case of adatoms. Experimentally, there are strong asymmetries for individual dimers, though averaged over all dimers and temperatures the three possible positions are quite equally distributed with $N_H = 1241$, $N_L = 1149$, and $N_R = 1211$ for 3601 clearly identifiable positions. In the example shown in Fig. 5(a) only two positions are observed for 20 consecutive images (1900 s), i.e., as long as the third atom stays close by [22]. Thus, a third atom changes the rotation potential of the quantum rotor.

Figure 5(b) compares the number of observations of the three positions H, R, and L to the distance of the next nearest neighboring atom. For a random rotation, the difference in occurrence should remain constant. This is not the case in two regions in Fig. 5(b) (marked with vertical lines). In the first region $R_1$ ( $\sim$ image 50), the position R occurs *less* often than expected; in the second region $R_2$ ( $\sim$ image 160), the position H occurs *more* often than expected. The atom closest to the dimer is at a distance of $\sim$2.5 nm ( = 8.7 a) and $\sim$1.3 nm ( = 4.5 a) in regions $R_1$ and $R_2$, respectively. In general, we find the strongest influence of atoms on the dimer rotation, if one atom is at a distance of $5(\pm 1)$ or $9(\pm 1)$ atomic distances. Depending on the distance and on the relative orientation of the atom to the dimer, either one position is stabilized as in $R_1$ or one position is destabilized as in $R_2$. This suggests that the average residence time of the quantum rotor in one position before it changes to one of the other

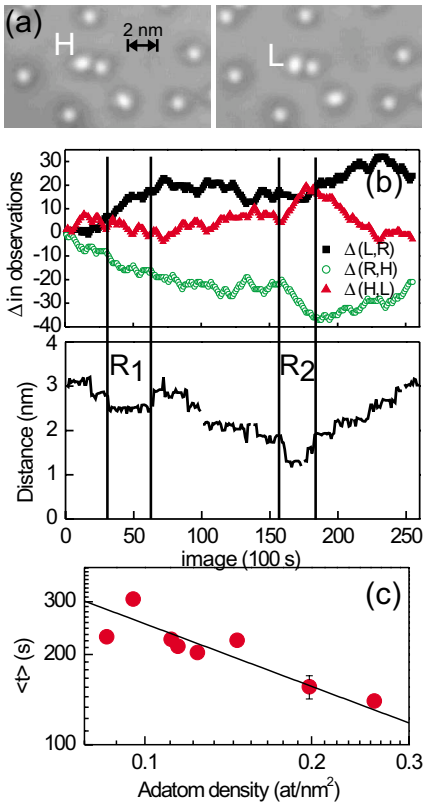


FIG. 5 (color online). Influence of atoms on dimer motion: (a) STM image: distance from dimer to atom $\Delta d = 1.08$ to 1.32 nm, $\Delta t = 100$ s, dimer positions: LLHHHHHLHHHHHHLHHHHH ($T = 20$ K, 203 mV, 0.43 nA) (b) The difference in the number of observations of rotational positions for a specific dimer at 20 K and the distance to the atom closest to it; for $\Delta(x, y) = -20$ position $y$ is observed 20 times less often than position $x$. (c) Average residence time $\langle t \rangle$ of a dimer in one of three equivalent positions during rotation vs local adatom density at 20 K.

two positions $\langle t \rangle$ depends on the (local) density of adatoms. Indeed, there is a power law dependence of $\langle t \rangle$ on adatom density [Fig. 5(c)].

In conclusion, we present a real space and real time dimer study on metals including formation, rotation, diffusion, and mutual long-range interaction with atoms via the surface state. For the case of Cu/Ag(111) the activation energies for atom diffusion, dimer rotation, and dimer diffusion are 80, 92, and 122 meV, respectively, in EMT calculations. In the experiment the activation energies for adatom and dimer diffusion are $(65 \pm 9)$ and approximately 73 meV, respectively. The energy difference between fcc and hcp sites is 5.5 meV. The qualitative results are not expected to be surface specific. However, by comparison to the homoepitaxial case, we have demonstrated that the decisive energies depend on the particular system. In contrast to semiconductor dimers, metal dimers retard growth [25]. Our investigation underscores the fact that a deep understanding of diffusional properties and interaction of small adparticles beyond the atom is of utmost importance both experimentally and theoretically.

We acknowledge helpful discussions with Jascha Repp, IBM Zuerich, and financial support by the DFG through SFB 290 and SPP 1093.

[1] G. L. Kellogg, Surf. Sci. Rep. **21**, 1 (1994).
[2] H. Brune, Surf. Sci. Rep. **31**, 125 (1998).
[3] R. Gomer, Rep. Prog. Phys. **53**, 917 (1990).
[4] *Surface Diffusion: Atomistic and Collective Processes*, edited by M. C. Tringides (Plenum Press, New York, 1997).
[5] G. Ehrlich, Surf. Sci. **246**, 1 (1991); K. Kyuno and G. Ehrlich, Phys. Rev. Lett. **84**, 2658 (2000); S. C. Wang, G. Ehrlich, Phys. Rev. B **65**, 121407 (2002).
[6] P. J. Feibelman, Phys. Rev. Lett. **58**, 2766 (1987).
[7] T. R. Linderoth *et al.*, Phys. Rev. B **61**, R2448 (2000); T. R. Linderoth *et al.*, Surf. Sci. **402**, 308 (1998).
[8] T. Mitsui *et al.*, Science **297**, 1850 (2002).
[9] e.g. K. Morgenstern, G. Rosenfeld, B. Poelsema, and G. Comsa, Phys. Rev. Lett. **74**, 2058 (1995); W. W. Pai, A. K. Swan, Z. Zhang, and J. F. Wendelken, Phys. Rev. Lett. **79**, 3210 (1997); D. C. Schlößer *et al.*, Surf. Sci. **465**, 19 (2000).
[10] G. Boisvert and L. J. Lewis, Phys. Rev. B **59**, 9846 (1999).
[11] M. Vladimirova, A. De Vita, and A. Pimpinelli, Phys. Rev. B **64**, 245420 (2001).
[12] A. Bogicevic, P. Hyldgaard, G. Wahnström, and B. I. Lundqvist, Phys. Rev. Lett. **81**, 172 (1998).
[13] T. Einstein, in *Physical Structure of Solid Surfaces*, edited by W. N. Unertl (North-Holland, Elsevier, 1996).
[14] A. Bogicevic, Phys. Rev. Lett. **82**, 5301 (1999).
[15] A. Bogicevic *et al.*, Phys. Rev. Lett. **85**, 1910 (2000).
[16] J. Repp *et al.*, Phys. Rev. Lett. **85**, 2981 (2000).
[17] T. R. Linderoth *et al.*, Phys. Rev. Lett. **78**, 4978 (1997); T. R. Linderoth *et al.*, Phys. Rev. Lett. **82**, 1494 (1999); R. van Gastel *et al.*, Phys. Rev. Lett. **86**, 1562 (2001).
[18] N. Knorr *et al.*, Phys. Rev. B **65**, 115420 (2002).
[19] K.-F. Braun, Ph.D. thesis, Freie Universität Berlin, 2001.
[20] K. Morgenstern, G. Rosenfeld, B. Poelsema, and G. Comsa, Surf. Sci. **352–354**, 965 (1996).
[21] P. Stoltze, J. Phys. Condens. Matter **6**, 9495 (1994). Though the absolute values might have an uncertainty of $\approx 10\%$, the order of the processes is well presented. For instance, the calculated diffusion energy for a Cu monomer on Cu(111) is with 54 meV in fair agreement with the recent DFT calculation of 50 meV [15] as well as the energy for dissociation with 0.35 eV as compared to 0.38 eV calculated based on the transition state theory [U. Kürpick, Phys. Rev. B **66**, 165431 (2002)].
[22] http://www.physik.fu-berlin.de/~kmorgens/filme.html
[23] K. Morgenstern and K.H. Rieder (to be published).
[24] C. M. Chang, C. M. Wei, and S. P. Chen, Phys. Rev. B **54**, 17083 (1996).
[25] R. A. Wolkow, Phys. Rev. Lett. **74**, 4448 (1995); R. M. Tromp and M. Mankos, Phys. Rev. Lett. **81**, 1050 (1998); H. J. W. Zandvliet, T. M. Galea, E. Zoethout, and B. Poelsema, Phys. Rev. Lett. **84**, 1523 (2000).